Tribol Lett (2013) 52:395–405
DOI 10.1007/s11249-013-0223-x

ORIGINAL PAPER

Atomistic Simulation of Frictional Sliding Between Cellulose Iß Nanocrystals

Xiawa Wu · Robert J. Moon · Ashlie Martini

Received 25 June 2013/Accepted 16 September 2013/Published online: 1 October 2013

Abstract Sliding friction between cellulose Iß nanocrystals is studied using molecular dynamics simulation. The effects of sliding velocity, normal load, and relative angle between sliding surface are predicted, and the results analyzed in terms of the number of hydrogen bonds within and between the cellulose chains. We find that although the observed friction trends can be correlated with hydrogen bonding, it may not be the most significant factor in determining frictional behavior on cellulose nanocrystal surfaces.

Keywords Nanotribology · Polymers · Friction mechanisms · Dynamic modeling

1 Introduction

Cellulose nanocrystals (CNCs) are one of the most abundant nanomaterials in nature and recognized as a promising candidate to meet the growing demand for green, biodegradable, and sustainable nanomaterials in future applications [1, 26, 22]. CNCs are whisker-like nanoparticles typically 3–20 nm in diameter and 100–3,000 nm in length depending on their source [1]. This material has drawn significant interest because of its high axial elasticity and low density, characteristics that have been extensively studied over the years [20, 31, 10, 33, 36, 2].

In this research, we focus on the surface rather than the bulk material properties of CNCs. Surface properties are important because these materials have a high surface-to-bulk ratio which means that surface properties may be as significant, if not more significant, than bulk properties in determining observed behaviors. CNC surfaces are also critically important to their potential application as reinforcement materials in nanocomposites, in which surface features play a major role in determining composite performance [1, 22, 16]. Here, we investigate a specific surface feature, the frictional resistance to sliding between two CNCs.

To date, experimental friction measurements of cellulose materials have been performed at microscopic length scales using atomic force microscopy (AFM) in colloidal probe mode. In these experiments, a cellulose sphere (15–25 µm in diameter) is attached to the end of a tipless cantilever and slid on various substrate materials including regenerated cellulose (cellulose II), CNCs, silica, and mica, usually with the whole system emerged in various liquid media such as water or NaCl solution [35, 3, 32, 29, 30]. All of these studies reported an increase in friction force with normal load. In addition, they reported that friction is dependent on the surface chemistry [29], surface roughness [30], and scan length [35]. No previous study has focused on the sliding between two crystalline cellulose surfaces.

While experimental measurements give us the magnitude of frictional resistance to sliding and how it changes with controllable operating conditions, they cannot, to this point, provide information about the mechanisms

X. Wu (✉)
School of Mechanical Engineering, Purdue University, West Lafayette, IN, USA
e-mail: wu123@purdue.edu

R. J. Moon
Forest Products Laboratory, US Forest Service, Madison, WI, USA
e-mail: robertmoon@fs.fed.us

A. Martini
School of Engineering, University of California Merced, Merced, CA, USA
e-mail: amartini@ucmerced.edu

underlying that resistance. To address this issue, we use molecular dynamics (MD) simulation, which describes the evolution of atoms and molecules over time, to predict surface friction. With this tool, we can control conditions more tightly than in the corresponding experiment and "see" what is happening in the interface buried between the contacting surfaces during sliding [7]. MD simulation has been used to study the mechanical and thermal properties of CNCs for years [20, 31, 10, 33, 36, 2].

In the current study, MD simulations are used to investigate sliding between contacting cellulose Iß surfaces. This is, to our knowledge, the first reported MD simulation of CNC friction and the first study of friction between crystalline cellulose using any method. We focus on the effects of sliding velocity, normal load, and the relative angle between contacting cellulose Iß surfaces. We also characterize the role of hydrogen bonding following the suggestion that the frictional behavior of biomaterials is significantly affected by the formation and breaking of hydrogen bonds [12] and based on previous MD studies which showed that hydrogen bonds have a significant influence on the predicted mechanical properties of CNCs [10, 34]. We analyze observed trends in terms of the hydrogen bonding within and between the cellulose chains. Simulation results reveal important connections between frictional behavior and hydrogen bonding for sliding at CNC–CNC interfaces.

2 Materials and Methods

Cellulose is a linear chain polymer with the formula $(C_6H_{10}O_5)_n$ that consists of glucose repeat units; a stable natural crystal form, Iß, consists of cellulose chains in a monoclinic crystalline lattice. Snapshots of a single glucose repeat unit, a cellulose chain, and a cross section of the crystal Iß are shown in Fig. 1. The molecular model of a cellulose Iß crystal is based on the structure reported from an X-ray diffraction study (a = 0.7784 nm, b = 0.8201 nm, c = 1.0380 nm (chain direction), n = ß = 90°, and y = 96.5°) [25] using Materials Studio software. The model structure and elasticity were previously validated by direct comparison to experimental measurements [34]. We initially modeled sliding on three different surfaces, (110), (110) and (200), and found that the magnitude of the friction depends on the surface. However, the effects of load, velocity, and orientation do not change, i.e., these parameters affect friction on any surface in the same way. Therefore, the results shown in this paper correspond to the (200) surface, labeled in Fig. 1, which has been shown to be common in plant-based cellulose nanomaterials [11], and is ideal from a simulation perspective because the strong hydrogen bonding within layers provides

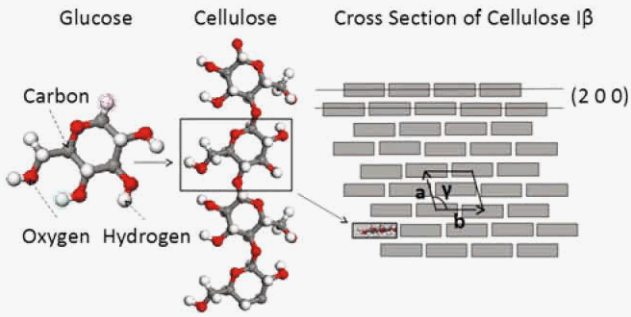

Fig. 1 Illustration of the construction of a model CNC. The leftmost image shows a glucose repeat unit the building block of cellulose. Carbon, oxygen, and hydrogen atoms are labeled: sphere sire is not representative of atomic dimensions. Glucose is connected through the $\beta(1 \rightarrow 4)$ link to form a linear cellulose chain as shown in the middle. The chains are assembled in the Iß crystal structure as shown on the right with the (200) surface labeled. The cross section of the crystal is defined by unit cell parameters a, b, and y

resistance to wear and surface damage that can occur during sliding.

The simulation system is a fully atomistic model that describes sliding between two cellulose Iß surfaces. The model components are shown schematically in Fig. 2a, where cellulose chains are represented by blocks. The cellulose substrate consists of two layers: top and bottom. The atoms in the bottom layer of the crystalline substrate are immobile to ensure a stable simulation system, and those in the top layer are free. The mobile cellulose is constrained such that it acts as a rigid body to which lateral velocity (V_{mc}) and normal force (N) can be applied. The boundaries in the x and z directions are periodic to model an infinitely large substrate, and a fixed boundary is used in the surface normal y direction. There are two potential sliding interfaces in the model the primary interface between the mobile cellulose and top substrate layer and the secondary interface between the two substrate layers. Figure 2b shows a schematic top view of the model where we define the reference axis along the chain direction of the substrate molecules, and 8 describes the angle between the chain direction of the mobile cellulose and the reference direction. When θ = 0°, the cellulose chains in the top substrate layer and the mobile cellulose are aligned. All simulations are conducted with LAMMPS software using the ReaxFF force field [9, 19]. ReaxFF is a reactive force field that explicitly describes covalent bonds, bond angles, bond angle torsion, van der Waals forces, Coulombic interactions, and hydrogen bonds. It has been successfully used to predict mechanical properties of CNCs [34].

First, a cellulose Iß crystal is equilibrated in the NPT (constant number of atoms, pressure, and temperature) ensemble at 300 K and 1atm using a Nod-Hoover

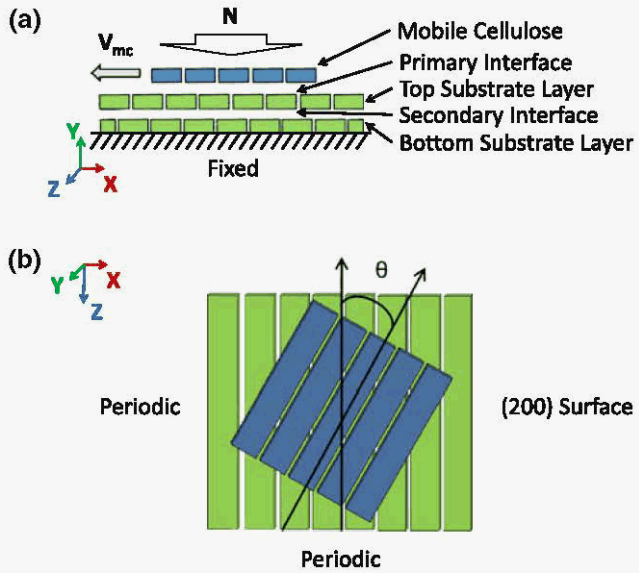

Fig. 2 **a** Illustration of the model components where blocks represent single cellulose chains. Periodic boundary conditions are applied in the x and z directions and a fixed boundary condition in the y direction. The mobile cellulose is constrained as a rigid body to which a lateral velocity V_{mc}, and a normal force N can be applied. **b** Top view of the mobile cellulose and the top substrate layer. The angle of the mobile cellulose with respect to the top substrate layer is θ

thermostat for 100 ps, relaxing both inner and outer constraints. Then, the (200) surface is chosen and placed facing the positive y direction serving as the substrate. The mobile cellulose is added to the model on top of the (200) surface at angle 8. The entire system is then equilibrated at 300 K in the NVT (constant number of atoms, volume, and temperature) ensemble for 10 ps. The first equilibration allows the CNC substrate to attain a stable configuration at room temperature, and the second equilibration allows the mobile cellulose to reach an equilibrium position above the substrate determined by the interfacial forces. The angle 8 does not change during equilibration.

After equilibration, the mobile cellulose is given a constant velocity V_{mc} in the negative x direction parallel to the surface; the other components of velocity (i.e., y and z) are unconstrained. The velocities applied in the simulation are much higher than those of typical AFM experiments. This limitation is due to the computational time required to model realistic systems. For example, it requires more than 200 h to simulate frictional sliding with a distance of 7.2 nm and 1 m/s sliding velocity for our CNC model containing about 6200 atoms. Previous research has shown that MD simulation can capture several key aspects of atomic-scale friction measured using AFM, despite the difference in velocities, but that direct comparisons must be made with caution [7]. Discussion of simulation results in the context of experimental measurements is presented in Sect. 3.5. A constant normal load N in the negative y direction is uniformly applied to all atoms in the mobile cellulose. The total sliding distance of the mobile cellulose is 7.2 nm. The lateral force on the mobile cellulose is recorded throughout the simulation. The maximum and minimum lateral forces are calculated by identifying the 99 and 1% of the ordered force data, respectively. The mean force is averaged over the entire sliding distance. Each simulation condition is repeated four times to calculate the average values and uncertainties. We analyze how the maximum and mean force varied with velocity of mobile cellulose (V_{mc}), normal load (N), and the orientation of the mobile cellulose with respect to the substrate (θ).

Intra- and interchain hydrogen bonding are considered to be very prevalent within the cellulose Iß (200) plane (named the "hydrogen-bonded' plane), in which the chains are strongly bonded to each other through hydrogen bonds [24, 23]. Also, studies of other hydrogen-bonded materials identified hydrogen bonding as one factor affecting friction at the nanoscale [12, 13]. It is therefore possible that hydrogen bonding also plays a role in sliding between our mobile cellulose and the substrate. To analyze this potential effect, we count the number of hydrogen bonds (N_{HB}) at the top and secondary interfaces, and within the top substrate layer using VMD software for each case. The cutoff distance and angle criteria used to define a hydrogen bond are 0.35 nm and 30°, respectively [18].

3 Results and Discussion

3.1 Friction Between CNCs

A typical lateral force profile is shown in Fig. 3 as a solid black line. Horizontal lines indicate the mean, maximum, and minimum forces, in this case calculated from the first 3.6nm of sliding. We observe a sawtooth pattern characteristic of stick-slip motion where the periodicity of the pattern reflects the lattice structures of the contacting materials.

As mentioned in the previous section, hydrogen bonding is believed to play a key role in the material properties of CNCs. To understand the effect of hydrogen bonding in sliding, we compare model predictions with hydrogen bonds "on" and "off," where hydrogen bonds are artificially removed by setting the cutoff distance to zero. Applying this criterion, no hydrogen bonds exist when the distance between hydrogen and oxygen atoms is greater than zero, which effectively removes all hydrogen bonds. This type of analysis has been performed before to understand the role of hydrogen bonding in the elastic properties of CNCs [10, 34]. Here, we analyze sliding for the case where V_{mc} = 50 m/s, N = 0 nN, and θ = 0°.

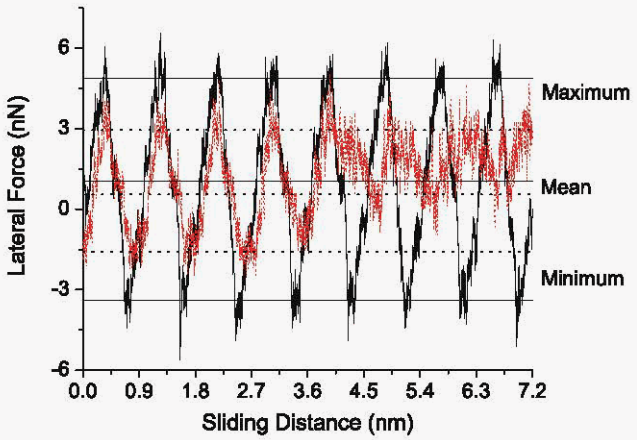

Fig. 3 The lateral frictional force with hydrogen bonds "on" (*solid black line*) shows a regular sawtooth pattern. The lateral force with hydrogen bonds "off" (*dotted red line*) has the same sawtooth pattern in the first 3.6 nm sliding distance but with smaller magnitude. This pattern is no longer observed in the last 3.6 nm of sliding because the surface is destroyed due to weakened molecular interactions caused by removal of hydrogen bonds. The *horizonal lines* indicate the mean, maximum, and minimum forces calculated from the first 3.6 nm of sliding. The simulation conditions are as follows: $V_{mc} = 50$ m/s, $N = 0$ nN, and $\theta = 0°$

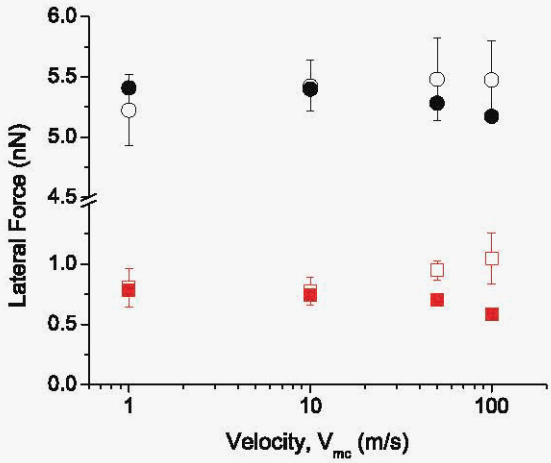

Fig. 4 The mean (*red squares*) and maximum (*black circles*) lateral forces are independent of sliding velocity (V_{mc}) when there is no constraint on the top substrate layer (*open symbols*). The *solid symbols* correspond to simulations where the center of mass of the top substrate layer is not allowed to move. The mean force in this case decreases with V_{mc} at large velocities. The forces at each V_{mc} are averaged over four trials to calculate the uncertainty. The simulation conditions are as follows: $N = 0$ nN and $\theta = 0°$

Figure 3 shows the lateral force with hydrogen bonds "off" as a dotted red line. We observe that the removal of hydrogen bonds decrease the mean lateral force by 34 % and the maximum force by 30 %. In addition, during the first 3.6 nm of sliding, the force both with and without hydrogen bonds exhibits stick-slip motion. This pattern continues throughout the sliding when hydrogen bonds are present. This is not the case, however, without hydrogen bonds after 3.6 nm of sliding. Analysis of snapshots from the simulation reveals that the surface structure is destroyed because the lack of hydrogen bonding weakened the molecular interactions in the top substrate layer. This case study suggests that the hydrogen bonding may be important in both friction and wear on CNC surfaces. Therefore, we will focus on analyzing the role hydrogen bonds play in the dependence of lateral force on velocity, normal load, and orientation in the following sections.

3.2 Velocity Effect

Friction on atomic scales is well known to be dependent on sliding velocity [28, 14, 27]. We study the effect of the velocity of the mobile cellulose (V_{mc}) over a range of values from 1 to 100 m/s. There is no external normal load applied on the mobile cellulose, and the angle θ is zero (chains in mobile cellulose and substrate aligned) in these simulations. The open symbols in Fig. 4 show the mean (red squares) and maximum (black circles) lateral force experienced by the mobile cellulose. The results indicate that there is no statistically significant relationship between lateral force and velocity V_{mc}. Similar velocity independence was reported for other hydrogen-bonded materials, which suggests that the system, at velocities employed in this paper, is far from the viscous linear-response regime [13].

To begin to understand these results, we consider where the relative motion occurs in our system. With the bottom substrate layer fixed and the mobile cellulose moving at a constant lateral velocity, there could be relative motion in the x direction at either the primary or secondary interfaces and both might contribute to frictional resistance. The inset of Fig. 5 shows the position of the center of mass (COM) of the top substrate layer in the x direction during the sliding process for the $V_{mc} = 50$ m/s case. The top substrate layer clearly exhibits oscillatory motion. The slope of the COM versus time curve when the top substrate layer is moving forward (obtained from a linear fit to the data as illustrated in the inset of Figure 5) is the velocity of that layer. The left y axis of Fig. 5 shows that the velocity of the top substrate layer (open black squares) increases with V_{mc}. The right y axis of Fig. 5 shows the contribution of the secondary interface to the total relative sliding velocity (solid red circles). An average value of $\sim$16% indicates that the majority of the relative motion occurs at the primary interface as expected, but that the contribution from the secondary interface is not negligible. In addition, the percent contribution of the relative velocity between substrate layers decreases marginally with increasing V_{mc}. This means that slightly more of the frictional resistance comes from the primary interface as V_{mc} is increased.

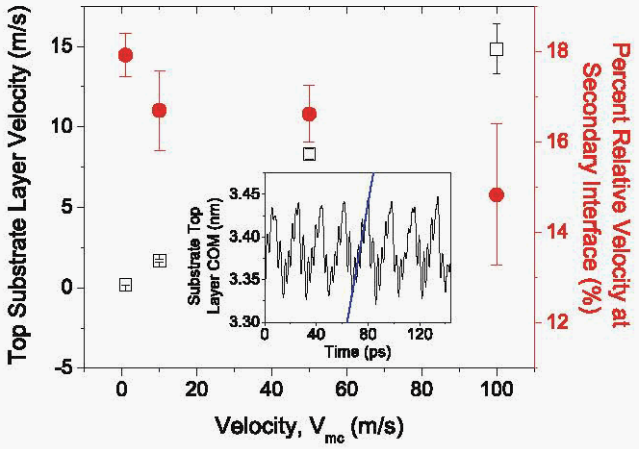

Fig. 5 The velocity of top substrate layer increases (*open black squares*, *left y* axis), and the percent of relative sliding that occurs between the two substrate layers decreases (*solid red circles*, *right y* axis) with sliding velocity V_{mc}. The *inset* shows the top layer velocity is calculated by a linear fitting to a plot of the COM of the top substrate layer versus time. The velocities at each V_{mc} are averaged over four trials to calculate the uncertainty. The simulation conditions are as follows: $N = 0$ nN and $\theta = 0°$

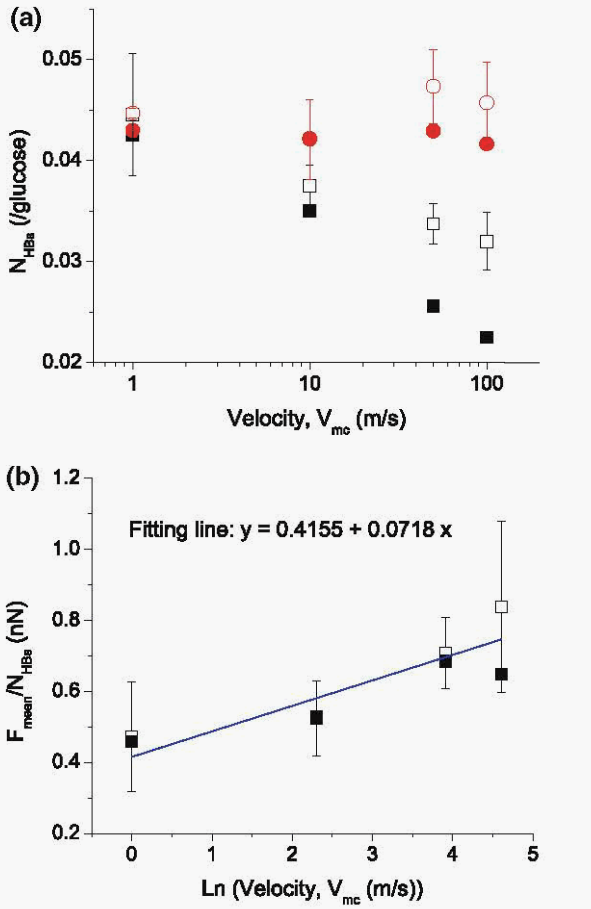

Fig. 6 **a** N_{HB} at the primary interface (*black squares*) decreases with sliding velocity V_{mc}, while N_{HB} at secondary interface (*red circles*) is not affected much. **b** Linear fitting of Eq. 1 with fit parameters $F_0 = 0.07$ nN and $V_0 = 0.003$ m/s. In both figures, the *open symbols* are from simulations with no constraints on the top substrate layer and the solid symbols from simulations where the COM of the top substrate layer is fixed. The N_{HB} and forces at each V_{mc} are averaged over four trials to calculate the uncertainty. The simulation conditions are as follows: $N = 0$ nN and $\theta = 0°$

To better understand the observed friction, we isolate the relative velocity at the primary interface by restricting the global motion of the top substrate layer, i.e., the center of mass is fixed, but the atoms are unconstrained. The resulting variations of mean and maximum lateral force are shown in Fig. 4 as solid symbols. For these cases, we observe a slight decrease in friction with V_{mc} where the magnitude of this decrease is statistically significant for the mean friction. Decrease in friction with velocity has been observed previously in AFM measurements on surfaces terminated by functional groups and attributed to the role of hydrogen bonding [5]. It was suggested that at low velocity, after stress release by a slip event, hydrogen bond networks can reform and again resist motion. However, fast sliding velocities do not allow sufficient time for this process to occur, and therefore, the friction is lower [5].

To further analyze the suggestion that a decrease in friction with velocity is related to hydrogen bonding in the interface, we calculate N_{HB} per glucose averaged over the entire sliding distance; the results are shown in Fig. 6a. We observe that N_{HB} at the primary interface (both open and solid black squares) decreases with V_{mc}; the faster the mobile cellulose moves, the fewer hydrogen bonds are formed between it and the top substrate layer. The trend is more significant when the motion of the top substrate layer is restricted, and relative motion occurs only at the primary interface (solid black squares). The consistency of the decrease in N_{HB} with velocity in Fig. 6a and the decrease in mean lateral force with velocity in Fig. 4 support the suggestion that hydrogen bonding and friction are related to these systems. Figure 6a also shows that V_{mc} does not significantly affect N_{HB} at the secondary interface (red circles) indicating that hydrogen bonding at the primary interface is more significant in terms of velocity dependence.

It was shown previously in simulations of other hydrogen-bonded materials that frictional dependence on velocity can be related to hydrogen bonding [12]. In that work, a direct relationship between friction, velocity, and number of hydrogen bonds was proposed:

$$F_{mean}/N_{HB} \approx F_0 ln(V_{mc}/V_0) = -F_0 lnV_0 + F_0 lnV_{mc}, \quad (1)$$

where F_{mean} is the mean lateral force, N_{HB} is the number of hydrogen bonds at the primary interface, and V_{mc} is the sliding velocity. We fit our data to this expression; the data and fit to Eq. 1 are shown in Fig. 6b. The fitting parameters from simulations with no constraints on the top substrate layer are $F_0 = 0.07$ nN and $V_0 = 0.003$ m/s, which are on

the same order of magnitude as those reported previously (F_0 = 0.019 nN and V_0 = 0.0023 m/s [12]). Fitting to data from simulations with the fixed top substrate layer yields similar values.

We have shown in Fig. 6a that N_{HB} decreases with sliding velocity whether the top substrate layer is fixed or not. However, we also observe in Fig. 4 that friction decreases with velocity only when the top substrate layer is fixed. This discrepancy can be explained by recalling that the velocity of the top substrate layer increases with V_{mc} as shown in Fig. 5. This increase is associated with an increase in friction because there are more avenues for energy dissipation when the top substrate layer is mobile. We verified the correlation between mobility, energy dissipation, and friction by calculating the energy dissipation rate at the fastest velocity (100 m/s) from simulations with and without top substrate layer mobility. The energy dissipation rate is 44 % larger when the top substrate is mobile. Therefore, the observation that there is no dependence on velocity for the free top substrate layer case can be attributed to the opposing effects of the increasing top substrate velocity (which increases friction) and decreasing number of hydrogen bonds (which decreases friction).

In summary, we found that mean friction is independent of velocity, but that this behavior is the result of two mechanisms that had opposing effects on friction. First, increasing V_{mc} caused a decrease in N_{HB} at the primary interface, leading to a decreased mean lateral force. We quantified the role of hydrogen bonding by fitting the data to an expression that quantitatively relates velocity, hydrogen bonding, and friction force. Second, increasing V_{mc} increased the mobility of the top substrate layer, which caused an increased mean lateral force. These effects were isolated by restricting the motion of the top substrate layer, which resulted in a decrease of friction with velocity. The analysis revealed that both hydrogen bonding and top substrate layer mobility are factors in velocity dependence. However, the results do not preclude the possibility that other effects, for example, interatomic forces, besides hydrogen bonding, may play a role.

3.3 Load Effect

Normal load affects frictional sliding on any length scale, but the relationship between load and friction is particularly complicated on small scales where adhesion and atomic roughness can become a significant factors [17, 21]. Friction is typically reported to increase monotonically with load, although how quickly it increases appears to be dependent on a variety of material and operating conditions [7]. In our simulations, we apply normal forces between 0 and 40 nN directly to the atoms in the mobile cellulose. The velocity is constant at V_{mc} = 50 m/s and angle θ = 0°. As shown in Fig. 7, the lateral forces increases linearly with load where the slope, i.e., coefficient of friction (COF), is 0.06 and 0.22 when calculated from the mean (open black squares) and the maximum (open red circles) forces, respectively. The static COF (maximum force slope) is greater than the kinetic COF (mean force slope) as expected.

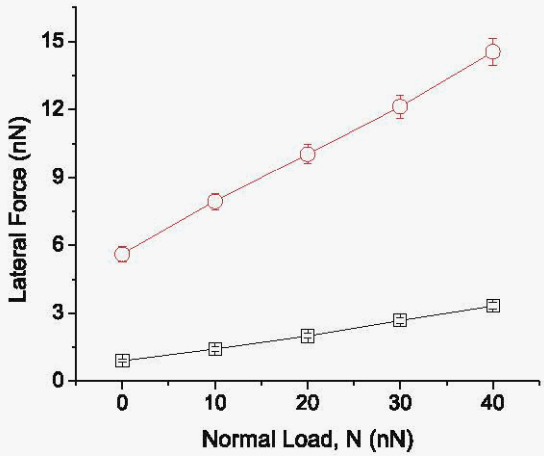

Fig. 7 The mean (open black squares) and maximum (open red circles) lateral forces increase linearly with normal load N with slopes of 0.06 and 0.22, respectively. The forces at each normal load are averaged over four trials to calculate the uncertainty. The simulation conditions are as follows: V_{mc} = 50 m/s and θ = 0°

In general, load can increase resistance to sliding by increasing the real area of contact or increasing the strength of the interaction between the two surfaces. For our simulation, the mobile cellulose size is fixed, so load only affects friction through the interatomic interaction. Interatomic interactions are a direct function of interatomic distance. It is therefore relevant to analyze the effect of load on the average interlayer distance at the primary and secondary interfaces (calculated as the distance in the z direction between the COM of two adjacent layers). Figure 8 shows that increasing the load from 0 to 40 nN causes the distance at the primary interface (open black squares) to decrease by -0.1nm, which is approximately 114 of the equilibrium distance between the two layers in a cellulose Iß crystal. The distance at the secondary interface (solid red circles) decreases only slightly. Note that, loads larger than 40 nN cause some of the covalent bonds in the cellulose molecules on the top substrate layer to break and with continued sliding, the substrate's structure is ultimately destroyed.

We also consider the effect of load in terms of hydrogen bonding. Figure 9a shows how N_{HB} varies with load. We observe that the N_{HB} at the primary interface (open black squares) increases with load N; this is consistent with the observation that the distance between layers decreases with the load (Fig. 8, open black squares), thereby allowing

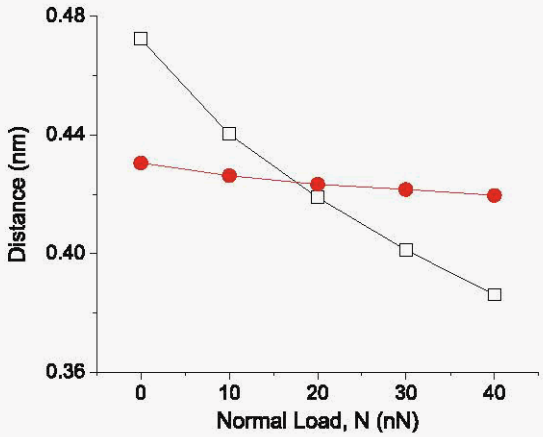

Fig. 8 As the normal load N increases, the distance of the primary interface (*open black squares*) decreases, while the distance of the secondary interface (*solid red circles*) is constant. The simulation conditions are as follows: $V_{mc} = 50$ m/s and $\theta = 0°$

more hydrogen bonds to form. The N_{HB} at the secondary interface (solid red circles) remains constant with load. As shown in the previous section, resistance to sliding comes from both interfaces. However, it appears that the effect of load is dominated by interactions at the primary interface. In general, the increase in N_{HB} with load agrees with previous simulations of hydrogen-bonded materials [12].

As shown in Fig. 9b, we also observe that increasing load causes a decrease in N_{HB} within the top substrate layer. This is consistent with the increase in N_{HB} in Fig. 9a: since there are a limited number of hydrogen atoms in the top substrate layer, the more hydrogen atoms that interact with the mobile cellulose and the bottom substrate layer, the less are available to form hydrogen bonds inside the layer. We also analyze the distribution of hydrogen bonds within and between chains in a given layer. At zero normal load, we find that the interchain hydrogen bonds are 29 % of the total N_{HB} in a layer, and the remainder are intrachain hydrogen bonds. Therefore, we observe that the largest N_{HB} is within individual cellulose chains, followed by the hydrogen bonds between chains in a given plane, with the least N_{HB} between neighboring "hydrogen-bonded" planes, which is in agreement with the distribution of hydrogen bonds observed in experiments [25].

In summary, the mean and maximum lateral forces on the cellulose Iβ (200) surface were found to be linear functions of normal load. This behavior was correlated with a decrease in the distance between layers at the primary interface with increasing load. The decreasing distance enabled more hydrogen bonds to form between all cellulose layers, which likely contributed to the increasing friction. The distance at the secondary interface was less affected by normal load. Finally, the increasing N_{HB} between layers corresponded to a decreasing N_{HB} within the layers.

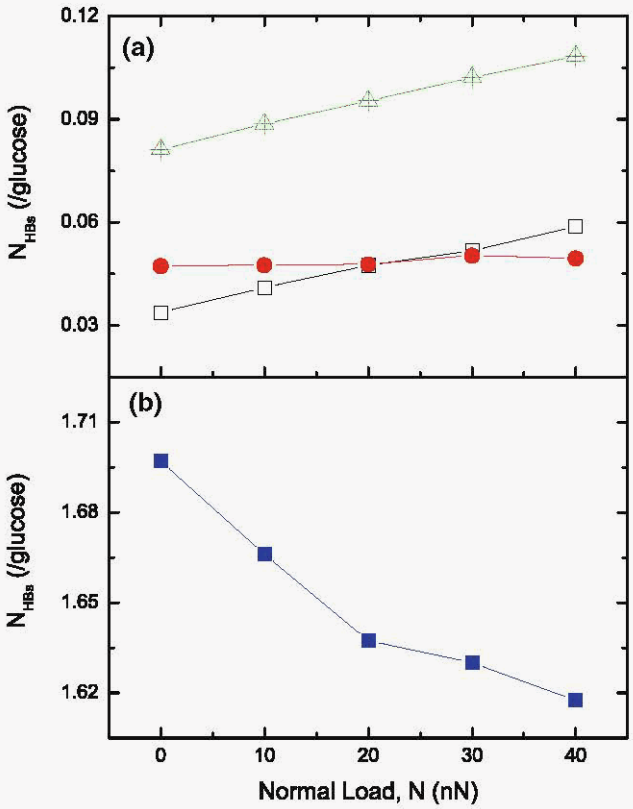

Fig. 9 **a** Increasing load causes an increase in the N_{HB} at the primary interface (*open black squares*), while the N_{HB} at the secondary interface (*solid red circles*) remains relatively constant. The total interfacial N_{HB} (*crossed green triangles*), which is a summation of the above two, thus increases. **b** Correspondingly, the N_{HB} within the top layer substrate decreases since the total number of hydrogen atoms is a constant. The simulation conditions are as follows: $V_{mc} = 50$ m/s and $\theta = 0°$

3.4 Orientation Effect

It has been shown that friction between ordered surfaces can be a function of the relative orientation of those surfaces. For example, orientation dependence has been observed in modeling and simulations of crystalline metals [37, 8] and graphene [15, 4] where high friction occurred when the lattices of the contacting surfaces are aligned or commensurate, while very low friction occurred at other orientations (misaligned or incommensurate contact). This phenomenon is also found in experiments; for example, AFM measurements showed very low friction is possible when graphite layers are incommensurate [6]. Although CNCs do not exhibit the perfect atomic order of graphite or pure metals, they are crystalline and therefore can be expected to exhibit some dependence on the orientation of the two sliding surfaces. We explore this effect in the simulation by changing the mobile cellulose angle θ with respect to the substrate from 0° to 360° with a 30° interval (see Fig. 2b). After initial rotation, the mobile cellulose is constrained to slide in the negative x direction, but without

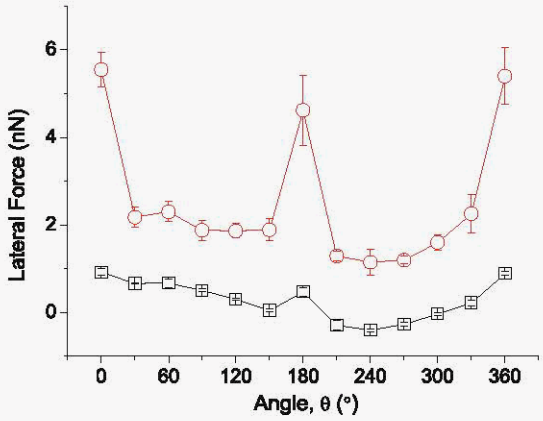

Fig. 10 The maximum (*open red circles*) and mean (*open black squares*) lateral forces are shown as functions of the relative angle θ between contacting surfaces. The forces at each angle are averaged over four trials to calculate the uncertainty. The simulation conditions are as follows: $V_{mc} = 50$m/s and $N = 0$ nN

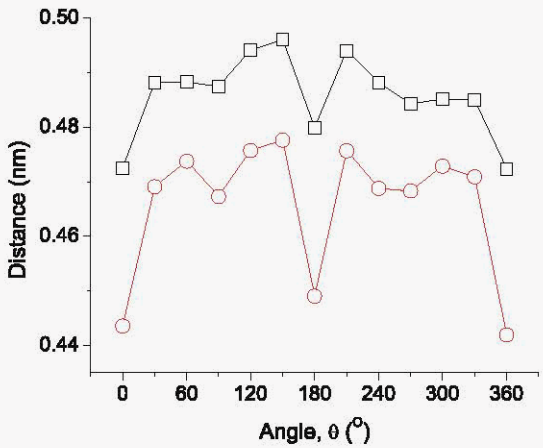

Fig. 11 The mean (*open squares*) and minimum (*solid circles*) distances of the primary interface at each angle θ are shown. The simulation conditions are as follows: $V_{mc} = 50$ m/s and $N = 0$ nN

further rotational movement. An external normal load of $N = 0$ nN and sliding speed of $V_{mc} = 50$ m/s are applied.

Figure 10 shows that the lateral forces varies with the angle θ. We observe that the maximum force (open red circles) and to a lesser degree the mean force (open black squares) are largest at angles of 0°, 180°, and 360°. At these three angles, the chains in the two contacting surfaces are perfectly aligned. For the other angles, where the chains are not aligned, the lateral forces are much lower. This result suggests that there are aligned and misaligned positions for sliding on cellulose Iβ surfaces.

As shown in the normal load section, the interlayer distance at the primary interface can be directly correlated with sliding resistance. The variation of the mean (open black squares) and minimum (solid red circles) distances with angle θ is shown in Fig. 11. The distances are at a minimum for the aligned ($\theta = 0°$, 180°, and 360°)

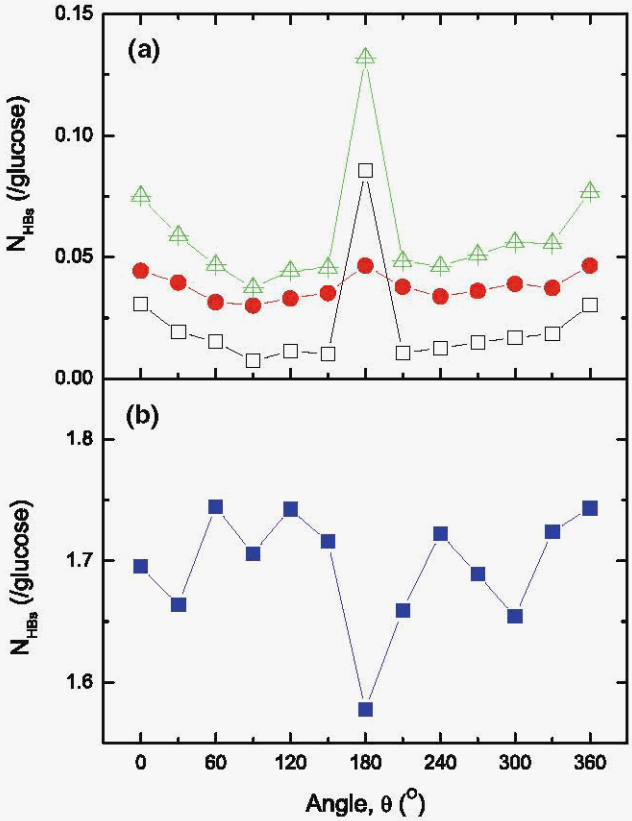

Fig. 12 **a** N_{HB} at the primary interface (*open black squares*), the secondary interface (*solid red circles*), and the summation of above two (*crossed green triangles*) vary with angle θ. **b** An opposite trend is observed for N_{HB} within the top layer substrate. In **a**, the interface N_{HB} exhibits a peak at 180°, which can be correlated with the valley in the intralayer N_{HB} at the same angle shown in **b**. The simulation conditions are as follows: $V_{mc} = 50$ m/s and $N = 0$ nN

positions. This is consistent with the force peaks in Fig. 10. For aligned angles, the mobile cellulose is closer to the top substrate layer during sliding, resulting in stronger interaction force and higher friction.

Although the friction is similar for the two aligned cases, 0° (or 360°) and 180° as seen in Fig. 10, analysis of the hydrogen bonding reveals some differences. Figure 12a shows there is a peak in N_{HB} at the primary interface at 180° (open black squares) that is more than three times larger than that at any other angle. The difference between the 0° and 180° configurations is the directionality of the chains. Figure 13 shows two different chain configurations, called parallel and anti-parallel based on the relative direction of the covalent bonds between *C*5 and *O*5. The "up" direction of a single cellulose molecule is defined to be from *C*5 to *O*5 as shown by the arrows in the top figure of Fig. 13. The term "parallel" is used when the cellulose chains are arranged such that they are all in "up" direction (as shown by M1 and M2), while "anti-parallel" describes alternating stacking of the cellulose chains (as shown by M2 and M3). The direction of the cellulose chain is

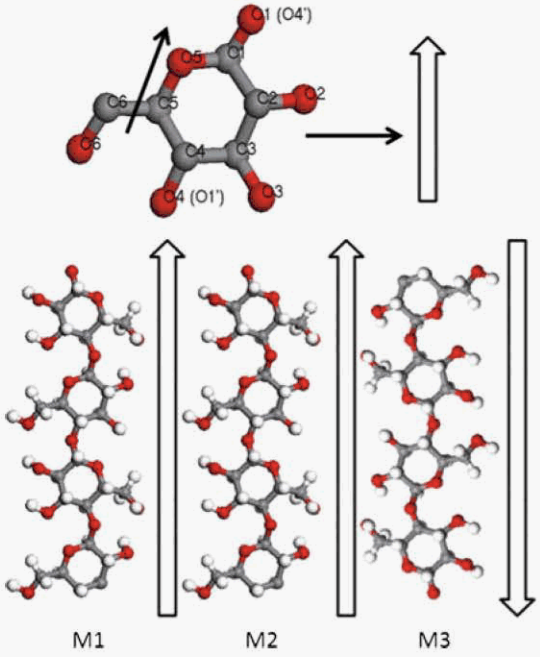

Fig. 13 The single glucose unit illustrates the "up" direction from atom *C5* to *O5*. Molecules *M1* and *M2* demonstrate the parallel configuration ($\theta = °$ and 360°), and *M2* and *M3* are in the anti-parallel configuration ($\theta = 180°$)

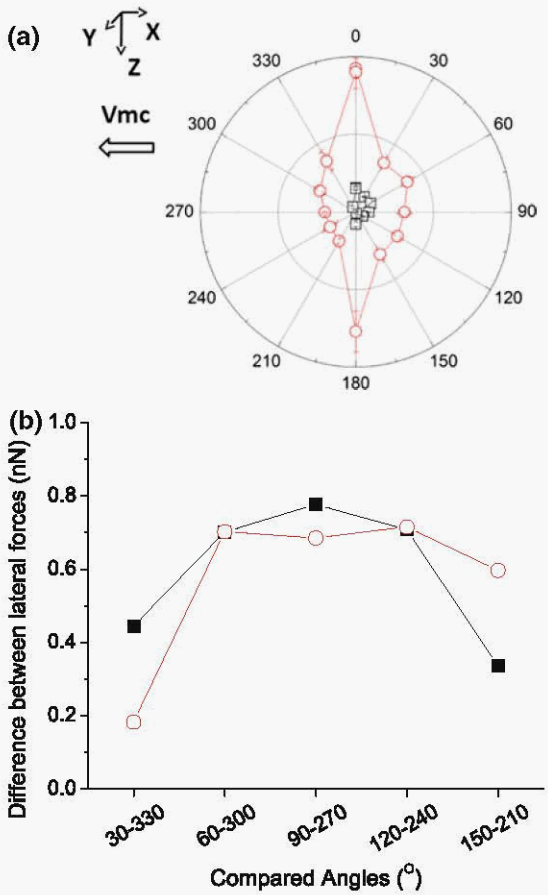

Fig. 14 **a** The mean (*open black squares*) and maximum (*open red circles*) lateral forces are functions of the relative angle θ and their magnitude is not symmetric about 180°. Siding is in the negative x direction, i.e. $\theta = 270°$. **b** The symmetric angles about 180° are paired up as shown on the x axis, and the difference of their averaged mean (*solid black squares*) and maximum (*open red circles*) lateral forces calculated. The force differences are most significant at 90°–270° which is apparently most affected by the sliding direction

important because it alters the interaction between neighboring hydrogen-bonded planes [22]. However, the effect of the parallel versus anti-parallel orientation on N_{HB} does not have an observable impact on mean and maximum lateral forces in Fig. 10. Note that, since the total number of hydrogen atoms is a constant in a single layer of substrate, the increased N_{HB} at 180° also corresponds to a decreased number of N_{HB} in the top substrate layer as shown in Fig. 12b.

Closer analysis of the misaligned orientations in Fig. 10 reveals that the lateral force is not symmetric about 180°. This is more clearly shown in Fig. 14, where Fig. 14a plots the friction radially to highlight the lack of symmetry, and Figure 14b illustrates the magnitude of the difference in friction at angles that are 180° apart. We observe that both the mean and maximum forces at angles between 0° and 180° are less than those at angles between 180° and 360°. This result suggests that another factor, the sliding direction, can affect friction. As mentioned previously and illustrated in Fig. 13, cellulose chains have a direction that is defined by the vector from atom *C5* to atom *O5*. This appears to affect fiction in misaligned contact. For example, the friction at 90° where the mobile cellulose slides in the "up" direction is greater than that at 270° where the sliding direction is opposite. At this point, we do not have direct evidence explaining the mechanism underlying this dependence, but further research could lead to new insights in the correlation between cellulose structure, surface properties, and sliding anisotropy at the CNC–CNC interface.

In summary, the relative orientation of the contacting cellulose surfaces was found to significantly effect friction and suggests that there may be sliding anisotropy at the CNC–CNC interface. As the orientation changes, the chains in the mobile cellulose and substrate come in and out of alignment. We found that the friction and the interface distance varied with relative angle, in the same way indicating a direct relationship. However, an analysis of the hydrogen bonding revealed that distance is not the only factor to be considered. For aligned surfaces, the chains might be parallel or anti-parallel. Although this difference significantly affected the N_{HB}, the effect on friction in aligned contact was negligible indicating that the interlayer distance is more significant in determining frictional behavior, and other atomic forces might dominate

the process. Finally, an analysis of the misaligned cases revealed a lack of symmetry that indicated sliding direction may also affect lateral force.

3.5 Relationship to Experiments

As mentioned in the Introduction, microscale friction experiments have been performed using colloidal probe AFM. The simulations of nanoscale sliding between two CNCs are not directly comparable to these experiments for several reasons: The experiments do not capture sliding between crystalline surfaces; experiments were performed in liquid environments; and, experimental length and time scales are larger than those accessible to the simulations. However, it is relevant to consider any similarities that may exist between results obtained using the two methods. Recall from the Sect. 3.2 that the simulations predicted no statistically significant effect of velocity on friction. This is consistent with the results of colloidal probe AFM measurements, which also showed no velocity dependence, albeit at much lower velocities (10^{-8} and 10^{-5} m/s) [35]. There is also consistency between experiment and simulation in the effect of load. First, both predict that friction increases linearly with normal load [29, 30]. Further, experiments performed with a very small scan length (10 nm) yielded a kinetic COF of 0.05 which is remarkably consistent with our simulation-predicted COF of 0.06 from a 7.2 nm scan length. Experiments with larger scan lengths (2 μm) reported COFs in the range of 0.41–1.18, which emphasizes the important role of length scale. Unfortunately, the orientation effect findings from simulation cannot be compared to experiment since alignment (and misalignment) is only possible with two crystalline materials. Despite the difference between the present simulations of nanoscale CNC–CNC contact and previous experiments using microscale colloidal probe AFM, the consistency of some trends in velocity and load dependence suggests that some of the mechanisms revealed by the simulation may be relevant on larger length scales and for more complex material combinations.

4 Conclusions

In summary, MD simulation was used to study the frictional resistance to sliding on cellulose Iß. We focused on the effect of velocity, load, and surface orientation on the mean and maximum lateral force and analyzed each of the observed trends in terms of N_{HB} formed between the contacting surfaces. These analyses revealed that there was some consistency between variations of friction with velocity, load, and orientation and the variation of N_{HB}. However, other effects were also identified including the mobility of the top substrate layer, direction of sliding relative to the chain orientation, and interlayer distance at the interfaces. These observations suggest that, although hydrogen bonding may play a role in sliding resistance on CNC surfaces, it may not be the most significant factor. This is supported by the observation that the total N_{HB} between layers at either the primary or secondary was small compared to that within individual chains and that some N_{HB} trends in (such as the dependence on parallel vs. anti-parallel orientation) do not appear to affect friction. The distance between layers at the primary interface is likely to be a key factor as it affects not only hydrogen bonding but also other interactions, such as van der Waals and Coulombic forces, whose strength also depends on interatomic distance. Although we did not explore these interactions here, their role may be significant, and further research to explore their contribution could provide additional insight into how sliding happens between two cellulose nanocrystals.

Acknowledgements The authors are grateful to financial support for this research provided by the Forest Products Laboratory under USDA Grant: 11-JV-11111129-087 – *Atomic-Scale Modeling of Cellulose Nanocrystals*, and Air Force Office of Sponsored Research Grant: FA9550-11-1-0162 *Thermal and Mechanical Properties of Nanocellulosic Materials: Integrated Modeling and Experiments.*

References

1. Azizi Samir, M.A.S., Alloin, F., Dufresne, A,: Review of recent research into cellulosic whiskers, their properties and their application in nanocomposite field. Biomacromolecules **6**(2), 612–626 (2005)
2. Bergenstråhle, M., Berglund, L.A., Mareau, K.: Thermal response in crystalline Iß cellulose: a molecular dynamics study. J. Phys. Chem. B **111**(30), 9138–9145 (2007)
3. Bogdanovic, G., Tiberg, F., Rutland, M.W.: Sliding friction between cellulose and silica surfaces. Langmuir **17**(19), 5911–5916 (2001)
4. Bonelli, F., Manini, N., Cadelano, E., Colombo, L.: Atomistic simulations of the sliding friction of graphene flakes. Eur. Phys. J. B **70**(4), 449–459 (2009)
5. Chen, J., Ratera, I., Park, J., Salmeron, M.: Velocity dependence of friction and hydrogen bonding effects. Phys. Rev. Lett. **96**(23), 236102 (2006)
6. Dienwiebel, M., Verhoeven, G.S., Pradeep, N., Frenken, J.W., Heimberg, J.A., Zandbergen, H.W.: Superlubricity of graphite. Phys. Rev. Lett. **92**(12), 126101 (2004)
7. Dong, Y., Li, Q., Martini, A.: Molecular dynamics simulation of atomic friction: A review and guide. J. Vac. Sci. Technol. A Vac. Surf. Films **31**(3), 030801–030801 (2013)
8. Dong, Y., Vadakkepatt A., Martini, A.: Analytical models for atomic friction. Tribol. Leu. **44**(3), 367–386 (2011)
9. Van Duin, A.C., Dasgupta S., Lorant, F., Goddard, W.A.: Reaxff: a reactive force field for hydrocarbons. l. Phys. Chem. A **105**(41), 9396–9409 (2001)
10. Eichhorn, S.J., Davies, G.R.: Modelling the crystalline deformation of native and regenerated cellulose Cellulose **13**(3), 291–307 (2006)

11. Elazzouzi-Hafraoui, S., Nishiyama, Y., Putaux, J.L., Heux, L., Dubreuil, F., Rochas, C.: The shape and sire distribution of crystalline nanoparticles prepared by acid hydrolysis of native cellulose. Biomacromolecules **9**(1), 57–65 (2007)
12. Erbaq, A., Horinek, D., Netz, R.R.: Viscous friction of hydrogen-bonded matter. J. Am. Chem. Soc. **134**(1), 623–630 (2011)
13. Erbaq, A., Netz, R.R.: Confinement-dependent friction in peptide bundles. Biophys. J. **104**(6), 1285–1295 (2013)
14. Gnecco, E., Bennewitz, R., Gyalog, T., Loppacher, C., Bammerlin, M., Meyer, E., Güntherodt, H.J.: Velocity dependence of atomic friction. Phys. Rev. Lett. **84**(6), 1172–1175 (2000)
15. Guo, Y., Guo, W., Chen, C.: Modifying atomic-scale friction between two graphene sheets: a molecular-force-field study. Phys. Rev. B **76**(15), 155429 (2007)
16. Kontturi, E., Tammelin, T., Österberg, M.: Cellulose-model films and the fundamental approach. Chem. Soc. Rev. **35**(12), 1287–1304 (2006)
17. Luan, B., Robbins, M.O.: The breakdown of continuum models for mechanical contacts. Nature **435**(7044), 929–932 (2005)
18. Luzar, A., Chandler, D.: Hydrogen-bond kinetics in liquid water. Nature **379**(6560), 55–57 (1996)
19. Mattsson, T.R., Lane, J.M.D., Cochrane, K.R., Desjarlais, M.P., Thompson, A.P., Pierce, F., Grest, G.S.: First-principles and classical molecular dynamics simulation of shocked polymers. Phys. Rev. B. 81(5), 054103 (2010)
20. Mareau, K., Heux, L.: Molecular dynamics simulations of bulk native crystalline and amorphous structures of cellulose. J. Phys. Chem. B **107**(10), 2394–2403 (2003)
21. Mo, Y., Turner, K.T., Szlufarska, I.: Friction laws at the nanoscale. Nature **457**(7233), 1116–1119 (2009)
22. Moon, R.J., Martini, A., Naim, J., Simonsen, J., Youngblood, J.: Cellulose nanomaterials review: structure, properties and nanocomposites. Chem. Soc. Rev. **40**(7), 3941–3994 (2011)
23. Nishiyama Y.: Structure and properties of the cellulose microfibril. J. Wood Sci. **55**(4), 241–249 (2009)
24. Nishiyama Y., Johnson, G.P., French, A.D., Forsyth, V.T., Langan, P.: Neutron crystallography, molecular dynamics, and quantum mechanics studies of the nature of hydrogen bonding in cellulose Iß. Biomacromolecules **9**(11), 3133–3140 (2008)
25. Nishiyama Y., Langan, P., Chanzy, H.: Crystal structure and hydrogen-bonding system in cellulose Iß from synchrotron X-ray and neutron fiber diffraction. J. Am. Chem. Soc. **124**(31), 9074–9082 (2002)
26. Postek, M.T., Vladar, A., Dagata J., Farkas, N., Ming, B., Sabo, R., Wegner, T.H., Beecher, J.: Cellulose nanocrystals the next big nano-thing?. Proc. SPIE **7042,** 70420D (2008)
27. Riedo, E., Gnecco, E., Bennewitz, R., Meyer, E., Brune, H.: Interaction potential and hopping dynamics governing sliding friction. Phys. Rev. Lett. **91**(8), 084502 (2003)
28. Sang, Y., Dubé M., Grant, M.: Thermal effects on atomic friction. Phys. Rev. Led. **87**(17), 174301 (2001)
29. Stiernstedt, J., Brurner, H., Zhou, Q., Teeri, T.T., Rutland M.W.: Friction between cellulose surfaces and effect of xyloglucan adsorption. Biomacromolecules **7**(7), 2147–2153 (2006)
30. Stiernstedt, J., Nordgren, N., Wågberg, L., Brurner III, H., Gray, D.G., Rutland M.W.: Friction and forces between cellulose model surfaces: a comparison. J. Colloid Interface Sci. **303**(1), 117–123 (2006)
31. Tanaka, F., Okamura, K.: Characterization of cellulose molecules in bio-system studied by modeling methods. Cellulose **12**(3). 243–252 (2005)
32. Theander, K., Pugh, R.J., Rutland, M.W.: Friction force measurements relevant to de-inking by means of atomic force microscope. J. Colloid Interface Sci. **291**(2), 361–368 (2005)
33. Wu, X., Moon, R.J., Martini, A.: Calculation of single chain cellulose elasticity using fully atomistic modeling. TAPPI J. **10**(4), 37-43 (2011)
34. Wu, X., Moon, R.J., Martini, A.: Crystalline cellulose elastic modulus predicted by atomistic models of uniform deformation and nanoscale indentation. Cellulose **20**(1), 43–55 (2013)
35. Zauscher, S., Klingenberg, D.J.: Friction between cellulose surfaces measured with colloidal probe microscopy. Colloids Surf. A **178**(1), 213–229 (2001)
36. Zhang, Q., Bulone, V., Ågren, H., Tu, Y.: A molecular dynamics study of the thermal response of crystalline cellulose Iß. Cellulose **18**(2), 207–221 (2011)
37. Zhang, Q., Qi, Y., Hector Jr, L.G., Çağın, T., Goddard III, W.A,: Atomic simulations of kinetic friction and its velocity dependence at Al/Al and $\alpha-Al_2O_3/\alpha-Al_2O_3$ interfaces. Phys. Rev. B **72**(4), 045406 (2005)